

Effects of the Velocity Waveform of the Physiological Flow on the Hemodynamics in the Bifurcated Tube

Hyung-Woon Roh, Jae-Soo Kim*

Chosun University, School of Aerospace, Naval Arch., & Ocean Engineering

Sang-Ho Suh

Soongsil University, Dept. of Mech. Engineering

The periodicity of the physiological flow has been the major interest of analytic research in this field up to now. Among the mechanical forces stimulating the biochemical reaction of endothelial cells on the wall, the wall shear stresses show the strongest effect to the biochemical product. The objective of present study is to find the effects of velocity waveform on the wall shear stresses and pressure distribution along the artery and to present some correlation of the velocity waveform with the clinical observations. In order to investigate the complex flow phenomena in the bifurcated tube, constitutive equations, which are suitable to describe the rheological properties of the non-Newtonian fluids, are determined, and pulsatile momentum equations are solved by the finite volume prediction. The results show that pressure and wall shear stresses are related to the velocity waveform of the physiological flow and the blood viscosity. And the variational tendency of the wall shear stresses along the flow direction is very similar to the applied sinusoidal and physiological velocity waveforms, but the stress values are quite different depending on the local region. Under the sinusoidal velocity waveform, a Newtonian fluid and blood show big differences in velocity, pressure, and wall shear stress as a function of time, but the differences under the physiological velocity waveform are negligibly small.

Key Words : Waveform, Physiological Flow, Sinusoidal Flow, Velocity, Pressure, Hemodynamic, Wall Shear Stress, Bifurcated Tube

Nomenclature

f : Periodic function
 p : Pressure [Pa]
 q : Index of Carreau model
 t : Time [s]
 u : Velocity vector [Pa]
 $\dot{\gamma}$: Shear rate [1/s]
 λ : Characteristic time [s]
 η : Apparent viscosity [Pa·s]
 η_0 : Zero shear rate apparent viscosity [Pa·s]
 η_∞ : Infinite shear rate apparent viscosity [Pa·s]

τ : Shear stress [Pa]

1. Introduction

Atherosclerosis is a disease which is related to way of life, with major risk factors being dietary fat and blood cholesterol, high blood pressure and smoking. Its harmful effects become apparent through occlusion of arteries, resulting in ischemia or infarction of tissues downstream. Atherosclerosis has its major ill-effects through restricting mean blood flow to particular organ. The influence of atherosclerosis is apparent in flow patterns in and beyond a stenotic lesion in an artery and in the pressure pattern downstream (Nichols et al., 1990). It is believed that atherosclerosis in the artery is related to the biochemical

* Corresponding Author,

E-mail : jskim@mail.chosun.ac.kr

TEL : +82-62-230-7080; **FAX :** +82-62-230-7139

Chosun University, School of Aerospace, Naval Arch., & Ocean Engineering. (Manuscript **Received** March 2, 2001; **Revised** September 27, 2002)

products that are released by the mechanical stresses and biochemical reaction on the arterial wall. The mechanical stresses of blood flow are transmitted to the wall by blood pressure, wall shear stresses and turbulent motion.

The periodicity of the physiological flow has been the major interest of analytic research in this field up to now (Milnor, 1989). However, interaction between blood flow and endothelial cells on the wall may be one of major factors in the pathogenesis of arterial disease. Among the mechanical forces stimulating the biochemical reaction of endothelial cells on the wall, the wall shear stresses show the strongest effect on the biochemical product. Pressure and wall shear stresses are related to the velocity waveform of the physiological flow and the blood viscosity. The physiological blood flow in the artery shows a periodicity but the velocity and pressure waveforms are very irregular. The objective of present study is to find the effects of velocity waveform on the wall shear stresses and pressure distribution along the artery and to present some correlation of the velocity waveform with the clinical observations.

2. Governing Equations and Waveform

2.1 Governing equations

The following continuity and momentum equations in index notation are used for the numerical analysis.

$$\frac{\partial u_j}{\partial x_j} = 0 \tag{1}$$

$$\rho \left(\frac{\partial u_i}{\partial t} + u_j \frac{\partial u_i}{\partial x_j} \right) = -\frac{\partial p}{\partial x_i} + \frac{\partial \tau_{ij}}{\partial x_j} \tag{2}$$

where ρ , p , u_i and τ_{ij} are density, pressure, velocity vector and shear stress tensor, respectively. The shear stress tensor in Eq. (2) may be expressed as a function of the shear rate as Eq. (3).

$$\tau_{ij} = \eta \left(\frac{\partial u_i}{\partial x_j} + \frac{\partial u_j}{\partial x_i} \right) \tag{3}$$

where η denotes the apparent viscosity.

A constitutive equation that expresses the apparent viscosity of blood as a function of the

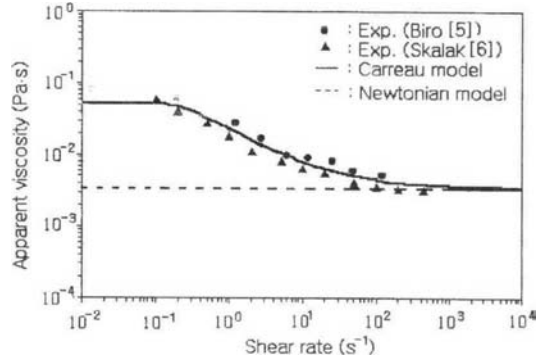


Fig. 1 Apparent viscosity of human blood as a function of the shear rate

shear rate is required to take into account the non-Newtonian viscosity of blood. Among many constitutive equations reported in the literature the Carreau model is used to express the apparent viscosity of blood as a function of the shear rate (Yoo et al., 1998 ; Benerjee, 1992).

$$\eta = \eta_\infty + (\eta_0 - \eta_\infty) [1 + (\lambda \dot{\gamma})^2]^{\frac{q-1}{2}} \tag{4}$$

where $\dot{\gamma}$, η_0 , and η_∞ denote the shear rate, the apparent viscosity at zero shear rate, and the apparent viscosity at infinite shear rate, respectively. λ and q in the model represent the characteristic time and index of the model, respectively. Rheological values of blood as a non-Newtonian fluid are taken to be $\eta_0 = 0.056 \text{ Pa}\cdot\text{s}$, $\eta_\infty = 0.00345 \text{ Pa}\cdot\text{s}$, and $\lambda = 3.313 \text{ s}$ and $q = 0.356$ based on the experimental data reported in the literature (Yoo et al., 1998). Experimental data and rheological models are presented in Fig. 1 (Biro, 1982 ; Skalak et al., 1981). For the first phase of numerical computation the blood viscosity is assumed as a Newtonian fluid with viscosity of $0.00345 \text{ Pa}\cdot\text{s}$, and for the second phase the viscosity is assumed as a non-Newtonian fluid with rheological values of the Carreau model described above.

2.2 Velocity waveform

2.2.1 Physiological velocity waveform

The abdominal aorta, the carotid arteries, the coronary arteries, and peripheral arteries such as the illiacs and the femoral are the favored sites for the development of atherosclerosis. The repeated

ejection of blood by the heart generates pressure and flow waves in the arteries and these pulsa-

tions are transmitted throughout the arterial tree. The traveling wave speed and the change in their shape and amplitude of waves are determined by the blood vessels, and differences of vascular size and distensibility throughout the system (Milnor, 1989).

Figure 2 shows the pressure and velocity waveform in the aorta and main branches recorded in a human body. Velocity in arteries was recorded by a catheter-tip electromagnetic flow meter.

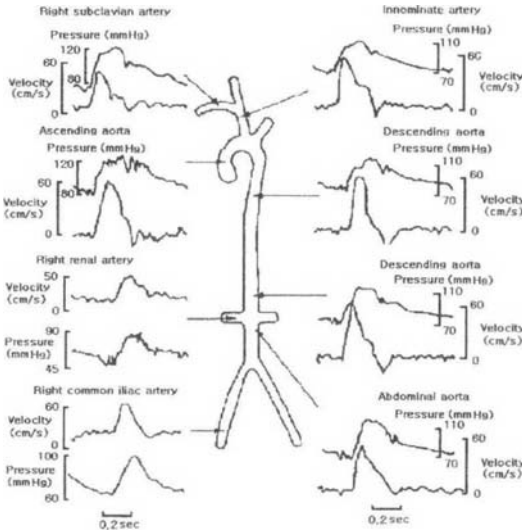


Fig. 2 Pressure and velocity waveforms in different arteries recorded in a human body

2.2.2 Sinusoidal waveform

The velocity waveforms in a human body are similar to the repetitive and asymmetric waveform as like physiological flow in the Fig. 2. Fortunately, these can be expressed numerically as the sum of sinusoidal waveform. Especially, the sinusoidal waveform is defined as the fundamental harmonic number ($k=1$) of physiological flow and is exerted a dominantly influence upon the flow pattern. Thus, in order to observation the

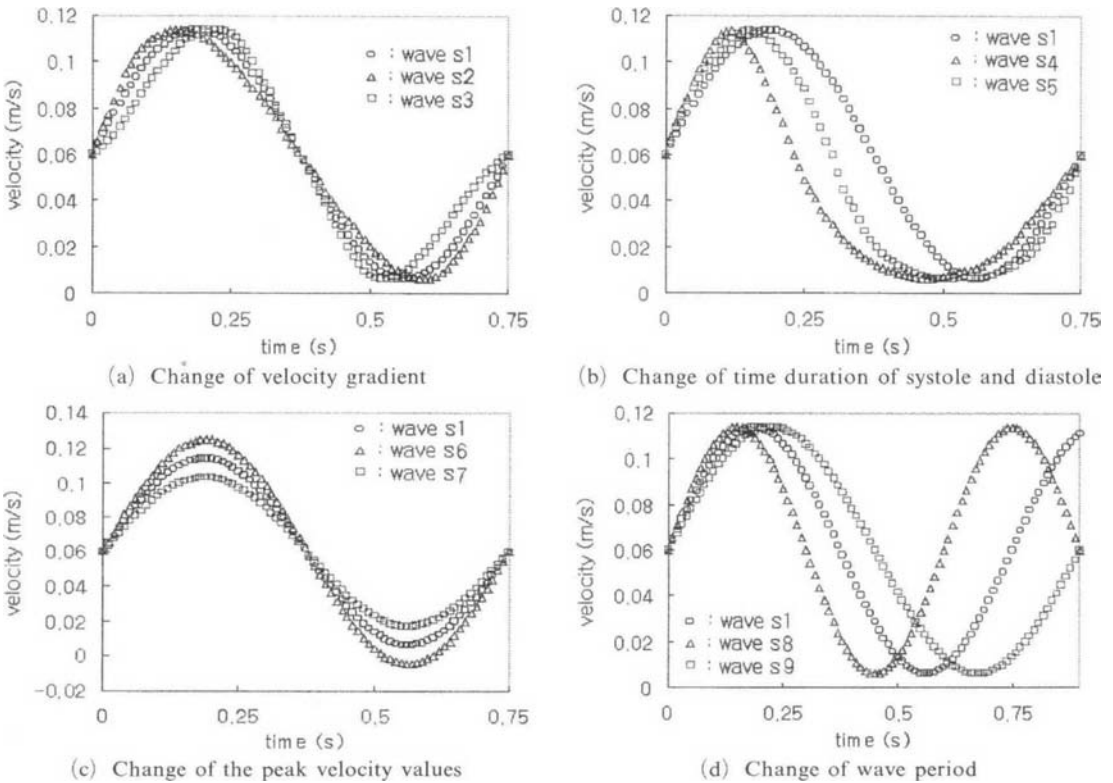


Fig. 3 Sinusoidal velocity waveform for numerical study

hemodynamic changes which it follows first in change of the waveform, these were simplified as sinusoidal waveform in Fig. 3.

In the present study four different groups of velocity waveform are selected to compute the velocity waveform effects on the wall shear stresses and pressure distribution.

Figure 3 shows four groups of velocity waveform: representing (a) change of velocity gradient for the same period, (b) change of time duration of systole and diastole for a given period, (c) change of the peak velocity values, and (d) change of wave period, so called the Wormersley number effect.

2.2.3 Simplified physiological waveform

The most effective way of expressing hemodynamic waveform numerically is by dissecting them into their component frequencies. The physiological velocity waveform of any shape is equivalent to the sum of a series of sinusoidal waves.

Under the steady-state oscillation any wave can be represented as the sum of a set of sinusoidal waves whose frequencies are all integral multiples of the frequency of repetition of the wave. Fourier's theorem states that any periodic function $f(t)$ is equal to the sum of an infinite series of terms.

$$f(t) = A_0 + \sum_{k=1}^{\infty} (A_k \cos k\omega t + B_k \sin k\omega t) \quad (5)$$

The sinusoid defined for $k=1$ is the fundamental harmonic and the second harmonic is described by the term when $k=2$, and so on.

In the present study four different groups of physiological velocity waveform are selected to compute the wall shear stresses and pressure distribution.

Figure 4 presents four groups of physiological velocity waveform: depicting (a) change of velocity gradient, (b) change of time duration of systole and diastole, (c) change of the peak ve-

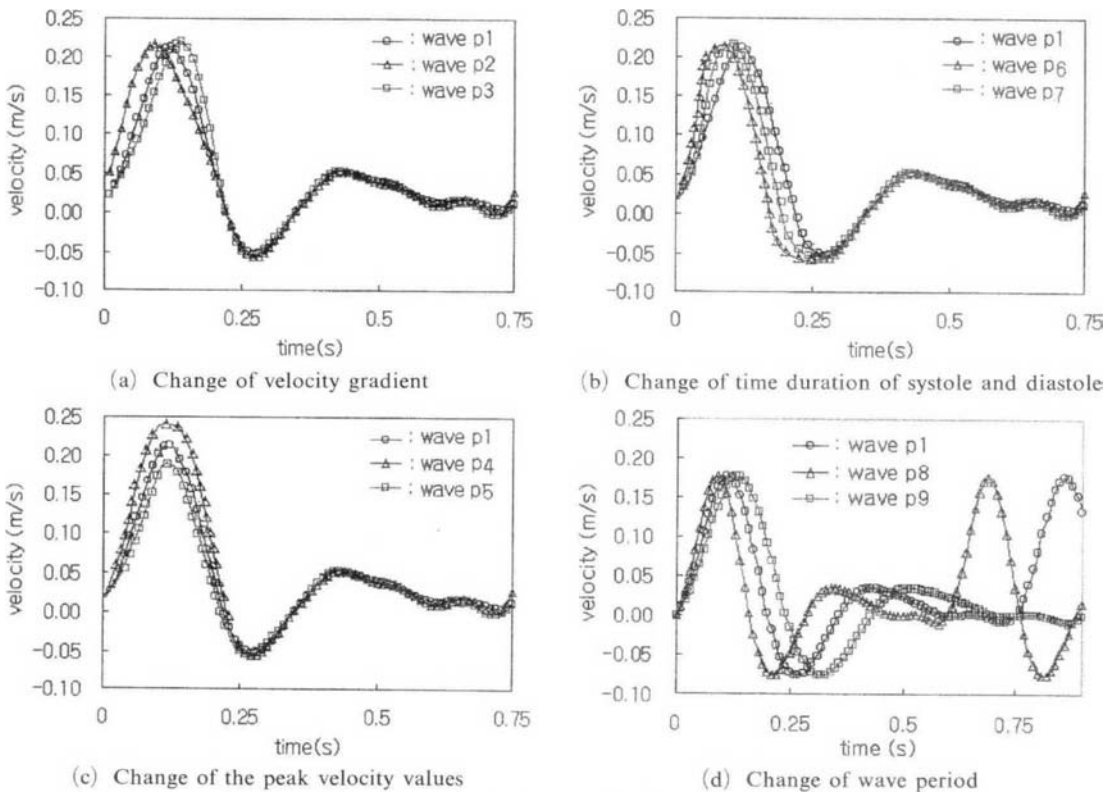


Fig. 4 Physiological velocity waveform for numerical study

locity values, (d) change of wave period, that is, the Wormersley number effect.

3. Flow Passage and Numerical Analysis

A straight circular tube whose inside diameter of 10 mm and 200 mm long and a bifurcated circular tube which is modelled for the femoral artery with inside diameter of 10 mm and bifurcation angle of 60 degrees are selected for the flow passages. Geometric shapes of the two flow passages are shown in Fig. 5.

The governing equations are discretized with non-staggered grid systems using finite volume method. In the non-staggered grid system the velocity components such as u , v , and w in the momentum equations are calculated for the same points that lie on the grid points of the pressure, p . This grid system not only simplifies the discretization equations but also reduces the memory spaces required for computation efficiently. However, it may bring out the checkerboard oscillation in the calculation of pressure field. Oscillating problem is removed by adapting Rhie-Chow algorithm (Rhie and Chow, 1983). The fully implicit scheme is utilized to solve the physiological flow problem, where time step is set to be 0.01 s. The HYBRID scheme is adapted for discretization of convective term and the SIMPLE

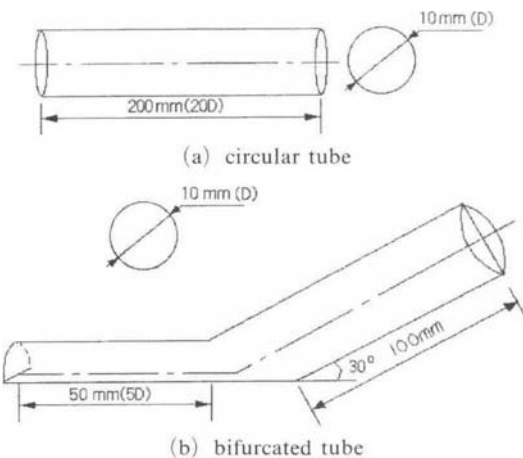


Fig. 5 Geometric shapes of the circular and bifurcated tubes

algorithm for treating pressure term in the momentum equations (Patankar, 1980; Yoo et al., 1996). The STONE method is used to obtain the iterative solution of the finite volume discretization equations (Stone, 1968).

In order to obtain the good solutions of transient flow, during the four cycles calculations are conducted and the convergence criteria is set to be 1×10^{-6} of the relative error to the flow velocity. The pressure boundary condition is imposed on the outlet boundary condition. It's used to the outflow boundaries where the surface pressure is known, but the detailed velocity distribution is not. This condition is suitable when it is desired to know the flow rate for a particular pressure drop across a piece of equipment (Yoo, et al., 1996; CFX 4. 1, User Manual, 1996).

4. Results and Discussion

4.1 Developing unsteady flow

For a given sinusoidal velocity waveform at inlet the velocity waveform in a tube varies its peak value depending on the axial and radial locations and time.

Figure 6 shows the developing unsteady velocity waveform along the centerline for a given fundamental velocity waveform applied at inlet. Due to the developing flow nature in a tube the peak velocity values exceed the velocity values at inlet resulting in the highest values at exit. For a given sinusoidal velocity waveform, the peak velocity values increase rapidly during the initial time step

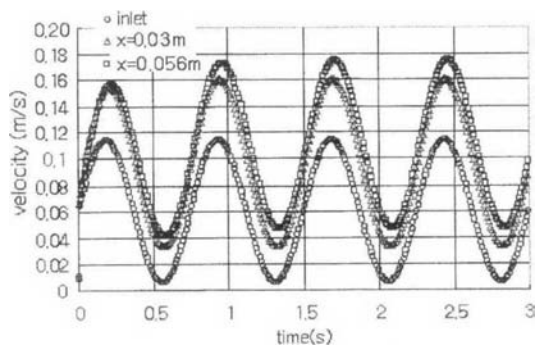


Fig. 6 Centerline velocity waveform for the developing unsteady flow

but asymptotically afterwards. It was found that the velocity waveform approaches the asymptotic peak value after four cycles showing the relative error of less than 0.08%, compared to the previous peak value. Table 1 presents the peak velocity values and the relative errors for the developing unsteady flow. For the following numerical study, four cycles of the velocity and pressure waveform are employed.

Table 1 Peak velocity and relative error for the developing unsteady flow

| period (cycle) | peak velocity (m/s) | relative error (%) |
|----------------|---------------------|--------------------|
| 1 | 0.1566 | reference |
| 2 | 0.1728 | 9.38% |
| 3 | 0.1744 | 0.92% |
| 4 | 0.1745 | 0.08% |

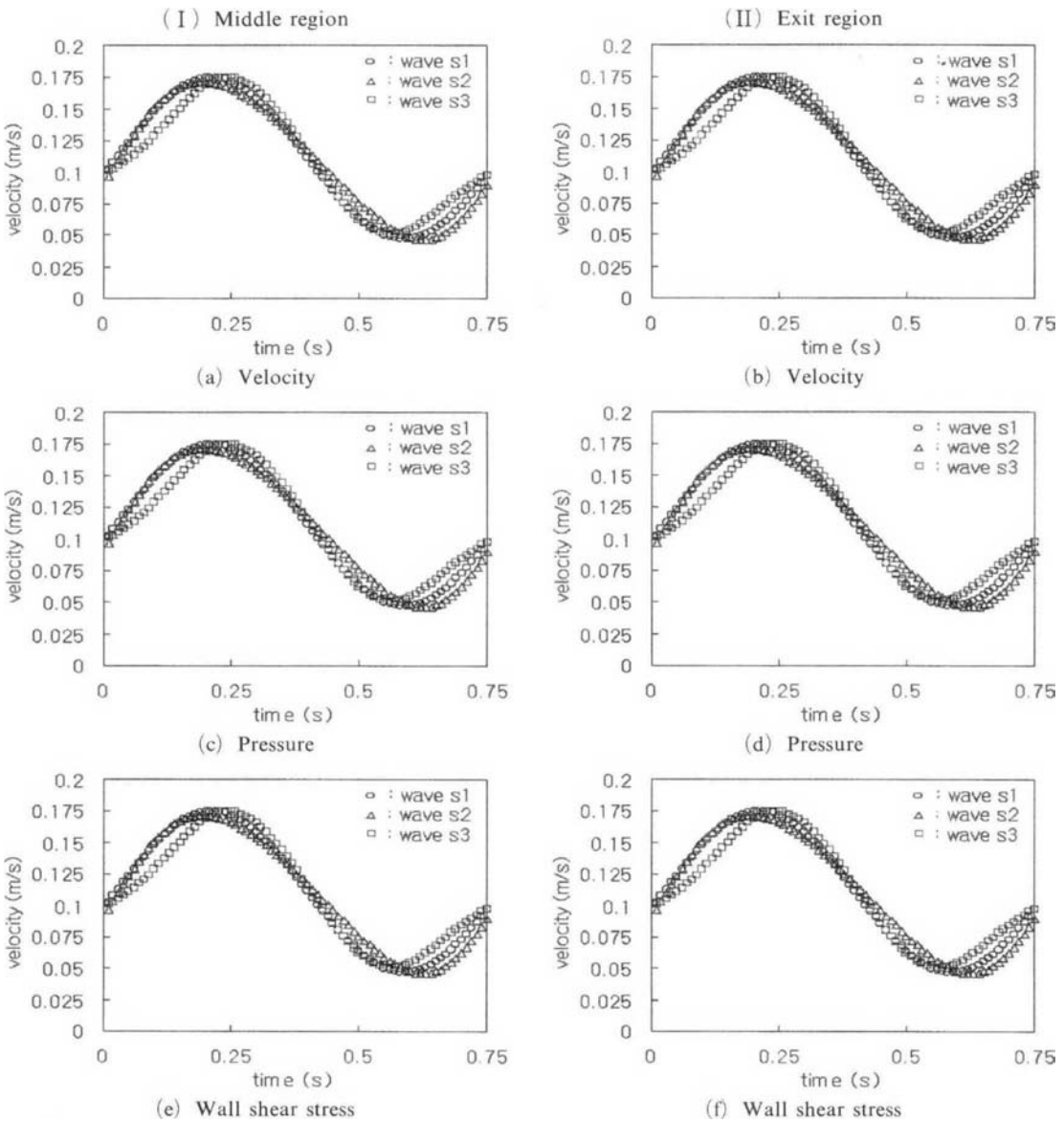


Fig. 7 Velocity, pressure, and wall shear stresses as a function of time for sinusoidal velocity waveform of s1, s2, and s3 at middle and exit regions of the circular tube

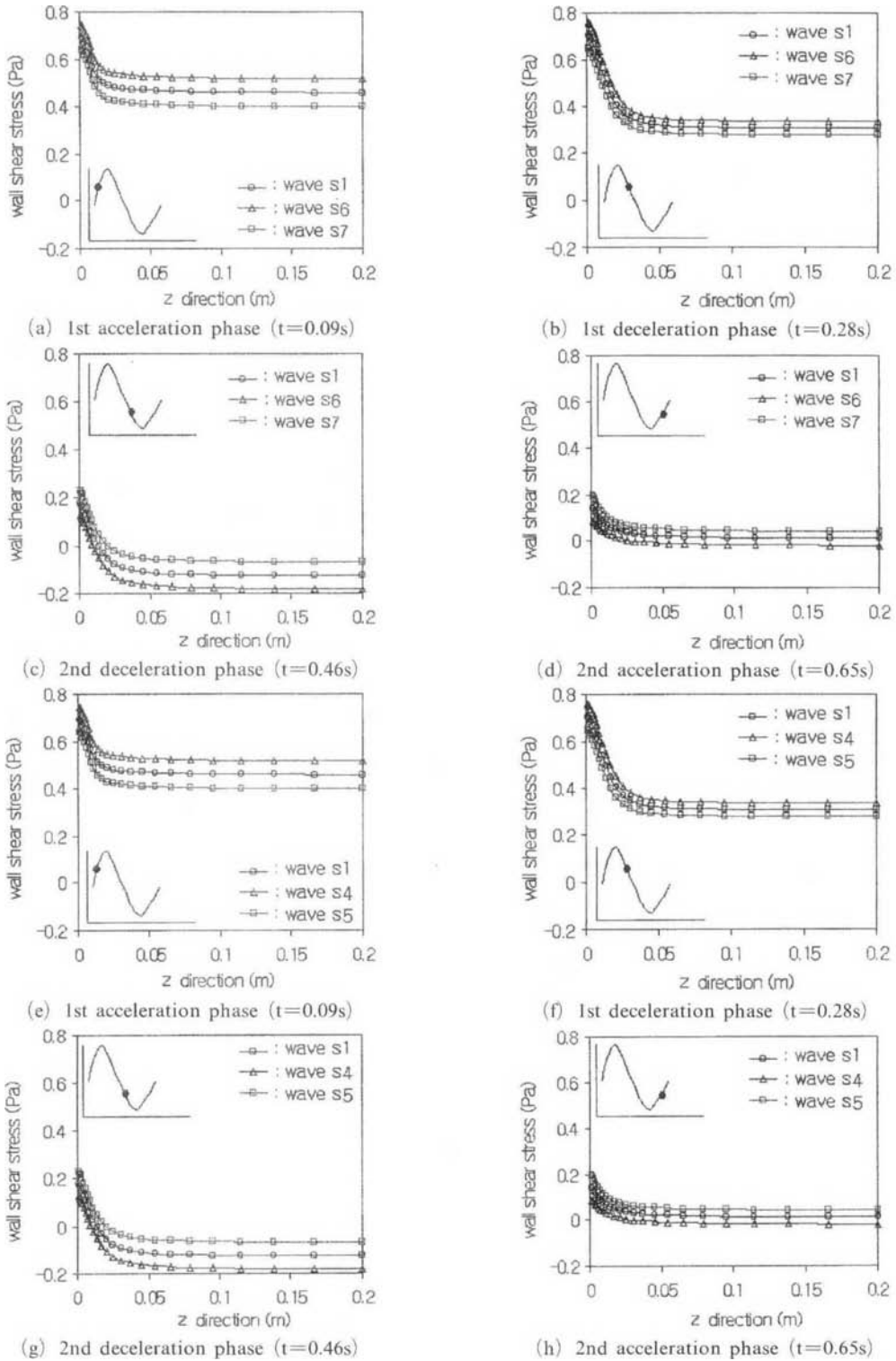


Fig. 8 Wall shear stress distributions along the flow direction for sinusoidal velocity waveform from s1 through s7 in the circular tube

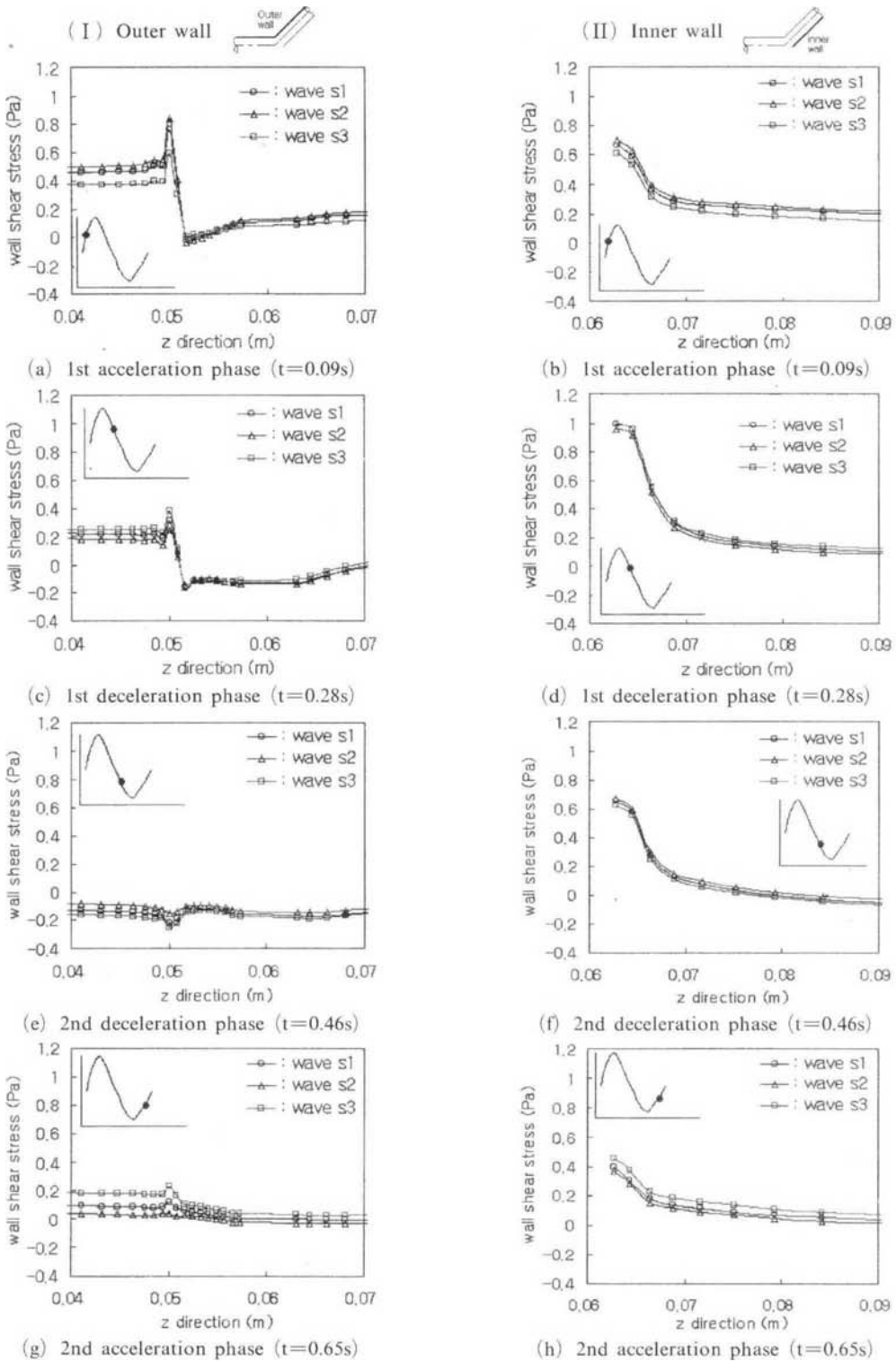


Fig. 9 Wall shear stress distributions along the flow direction for sinusoidal velocity waveform of s1, s2, and s3 in the bifurcated tube

4.2 Sinusoidal unsteady flow

In the present study wave s_i denotes the sinusoidal velocity waveform and velocity waves from $s1$ through $s9$ are employed for the analyses. Variations of velocity, pressure and wall shear stresses at middle and exit regions of the circular tube are presented in Fig. 7. The velocity waveform changes its shape very little, but the pressure waveform changes significantly. For a fluid of constant viscosity the wall shear stress is determined by the velocity gradient. The velocity profile of the flow changes its shape as the flow moves downstream and the same is true for the velocity gradient.

The wall shear stress distributions along the flow direction at specific time are presented in Fig. 8. The specific time of the sinusoidal waveform is as follows; the first acceleration time ($t=0.09s$), the first deceleration time ($t=0.28s$), the second deceleration time ($t=0.46s$), and the second acceleration time ($t=0.65s$). The variational tendency of wall shear stresses along the flow direction is very similar to the applied velocity waveform but the stress values are quite different depending on the local region. The highest values are recorded in the entrance region and the lowest values in the exit region.

The wall shear stresses decrease rapidly as flow develops in the entrance region and approaches to their asymptotic values. During the first acceleration and the first deceleration phases the wall shear stresses are positive values for all regions, while the second deceleration and the second acceleration phases the wall shear stresses are negative values in the developing region. Negative wall shear stresses imply that negative velocity prevails in the developed wall region during the second deceleration and second acceleration phases. Differences between the wall shear stresses for two waves are most pronounced during the second deceleration phase.

The wall shear stress distributions along the flow direction for sinusoidal velocity waveform of $s1$, $s2$, and $s3$ in the bifurcated tube are presented in Fig. 9. Change of the wall shear stress in a cycle may be an important factor for the mechano-transduction. Endothelial cells on the wall

experience the wall shear stresses during a cycle and biochemical reaction between the blood flow and cells is governed by the wall shear stresses. Most of research works about the interaction between the blood flow and endothelial cells are conducted in the steady flow chamber. Under the steady flow chamber endothelial cells experience a constant shear stresses, while endothelial cells of human arteries are exposed to the physiological unsteady shear stresses. Therefore, the physiological unsteady flow analysis and in vitro experiments under the unsteady flow condition should be conducted.

4.3 Physiological unsteady flows

In the present study of the physiological flows velocity wave p_i denotes the physiological unsteady velocity waveform and velocity waves $p1$ through $p9$ are employed for the analyses. Due to limitation of pages only a portion of results are presented in the paper.

Velocity, pressure, and wall shear stresses as a function of time for physiological velocity waveform of $p1$, $p2$, and $p3$ at middle and exit regions are presented in Fig. 10. The pressure waveform is quite different from the velocity waveform, but the wall shear stress waveform is very similar to the velocity waveform. The wall shear stress distributions along the flow direction for physiological velocity waveform from $p1$ through $p5$ are presented in Fig. 11. During acceleration phase ($t=0.07s$) velocity waveform of $p1$, $p2$, and $p3$ show quite big difference among different waveforms, meanwhile waveforms of $p1$, $p4$ and $p5$ show relatively small difference. During deceleration phase waveforms behave differently showing small difference among $p1$, $p2$, and $p3$ and big difference among $p1$, $p4$, and $p5$. These phenomena imply that the velocity gradient is dominant factor during acceleration phase and the peak values of the velocity waveform is prevalent factor during deceleration phase. The wall shear stress distributions along the flow direction for physiological velocity waveform of $p1$, $p2$, and $p3$ are presented in Fig. 12. Similar discussion may apply to the results of the bifurcated tube as discussed for the physiological waveform

in the circular tube.

4.4 Unsteady flows of non-newtonian fluids

In the present study for unsteady flows, effects of the blood on the velocity, pressure, and wall shear stress in the circular tube are analysed for the sinusoidal and physiological velocity waveforms. The analysis is concentrated for the gradi-

ent effects of the waveform.

Velocity and pressure of blood flow at middle and exit regions as a function of time for sinusoidal velocity waveform of s_1 , s_2 , and s_3 are presented in Fig. 13, and velocity and pressure waveforms for physiological velocity waveform of p_1 , p_2 , and p_3 are presented in Fig. 14. The velocity, pressure, and wall shear stresses of blood flow are very much similar to the results of

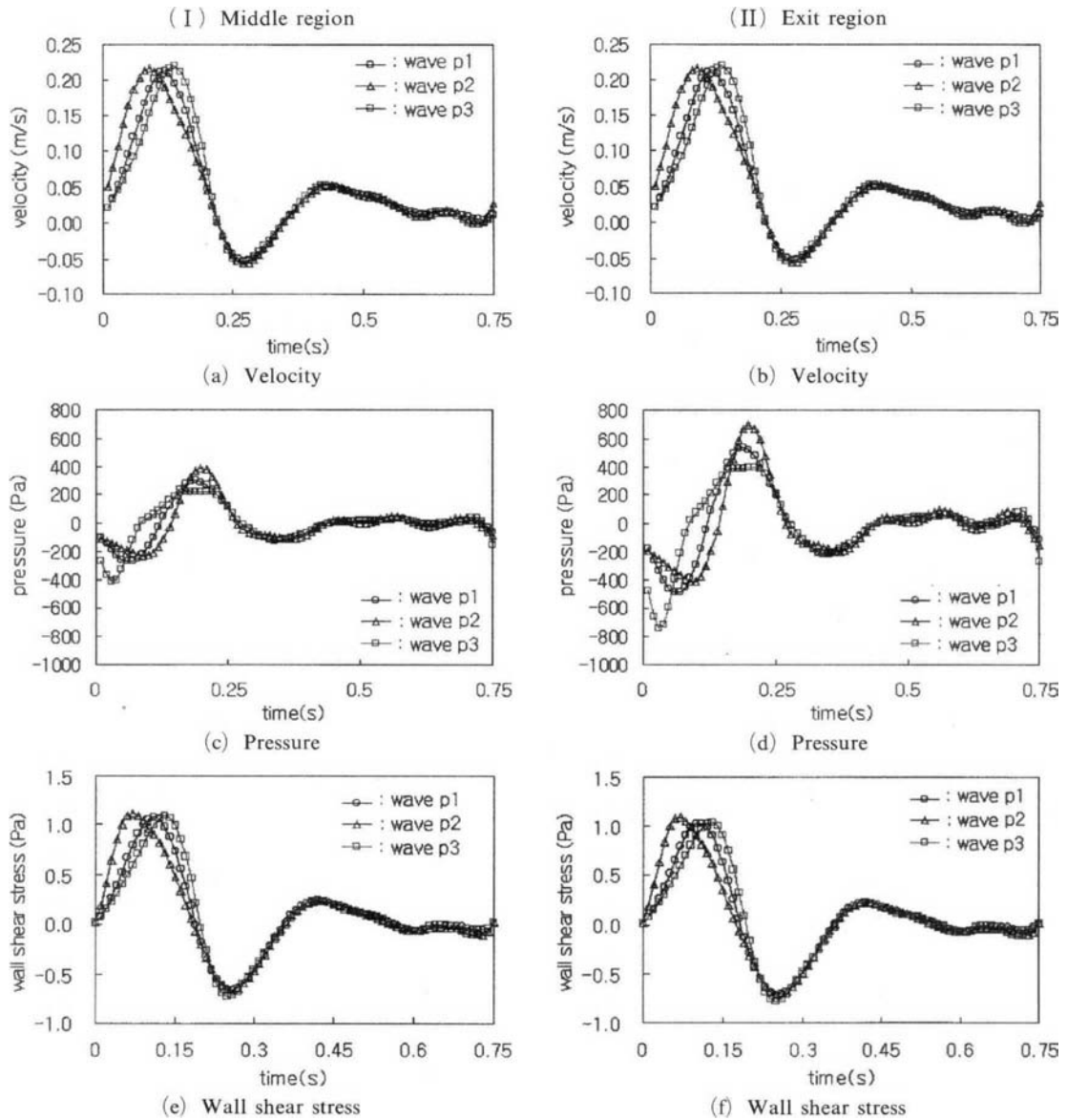


Fig. 10 Velocity, pressure, and wall shear stresses as a function of time for physiological velocity waveform of p_1 , p_2 , and p_3 at middle and exit regions of the circular tube

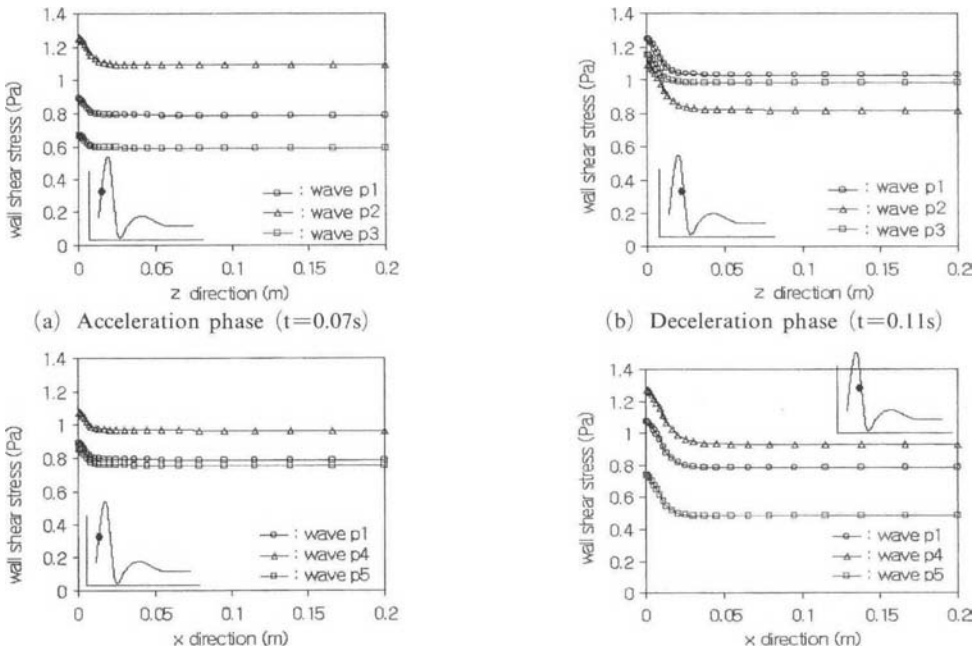


Fig. 11 Wall shear stress distributions along the flow direction for physiological velocity waveform from p1 through p5 in the circular tube

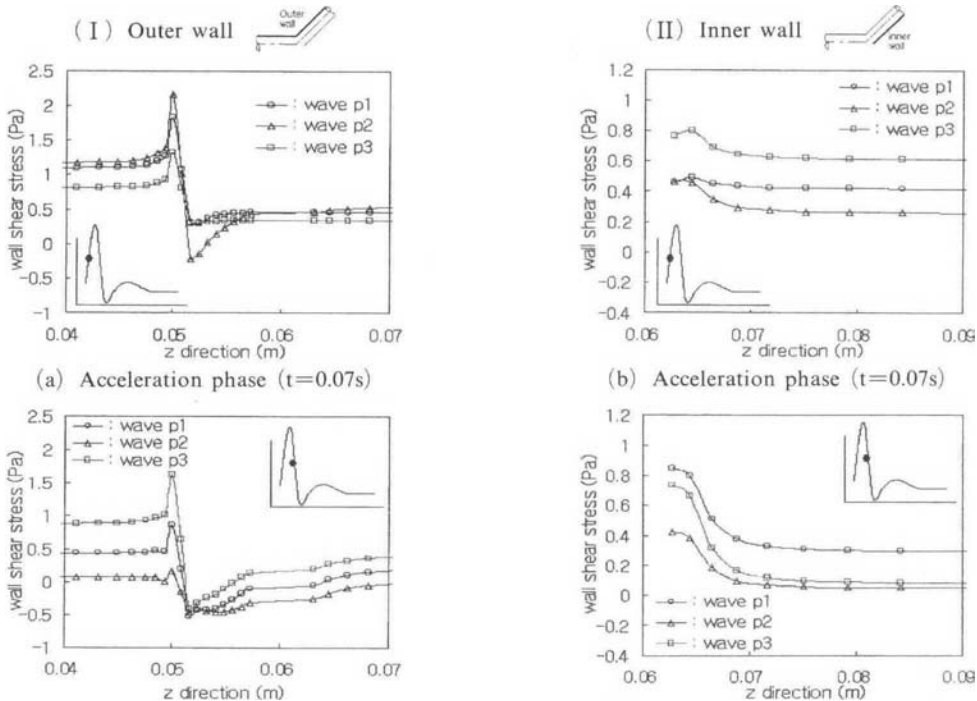


Fig. 12 Wall shear stress distributions along the flow direction for physiological velocity waveform of p1, p2, and p3 in the bifurcated tube

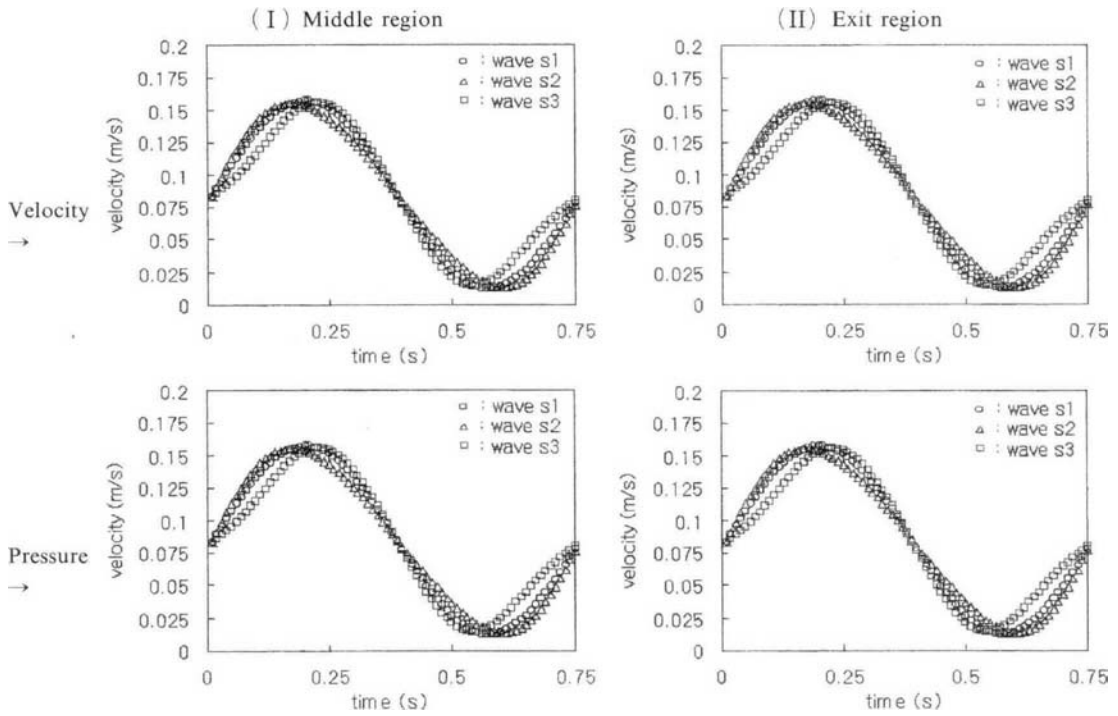


Fig. 13 Velocity and pressure of blood flow as a function of time for sinusoidal velocity waveform of s1, s2, and s3

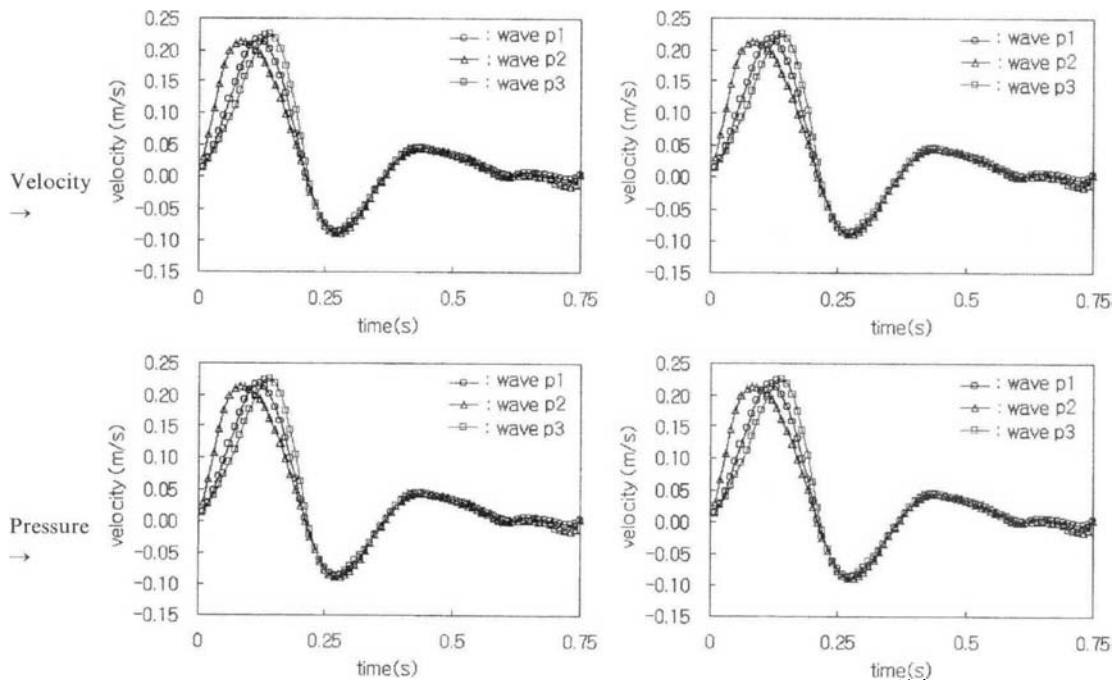


Fig. 14 Velocity and pressure of blood flow as a function of time for physiological velocity waveform of p1, p2, and p3

Newtonian fluid.

In order to differentiate the Newtonian fluid flow from blood flow the velocity waves $s1$ and $p1$ are taken as reference waveform and numerical results are compared on the same figure. Velocity, pressure, and wall shear stress for Newtonian fluid and blood as a non-Newtonian fluid are

presented in Fig. 15 for the sinusoidal velocity waveform of $s1$ and for the physiological velocity waveform of $p1$. Under the sinusoidal velocity waveform the differences in velocity, pressure, and wall shear stresses of two fluids are quite large, but the differences under the physiological velocity waveform are negligibly small.

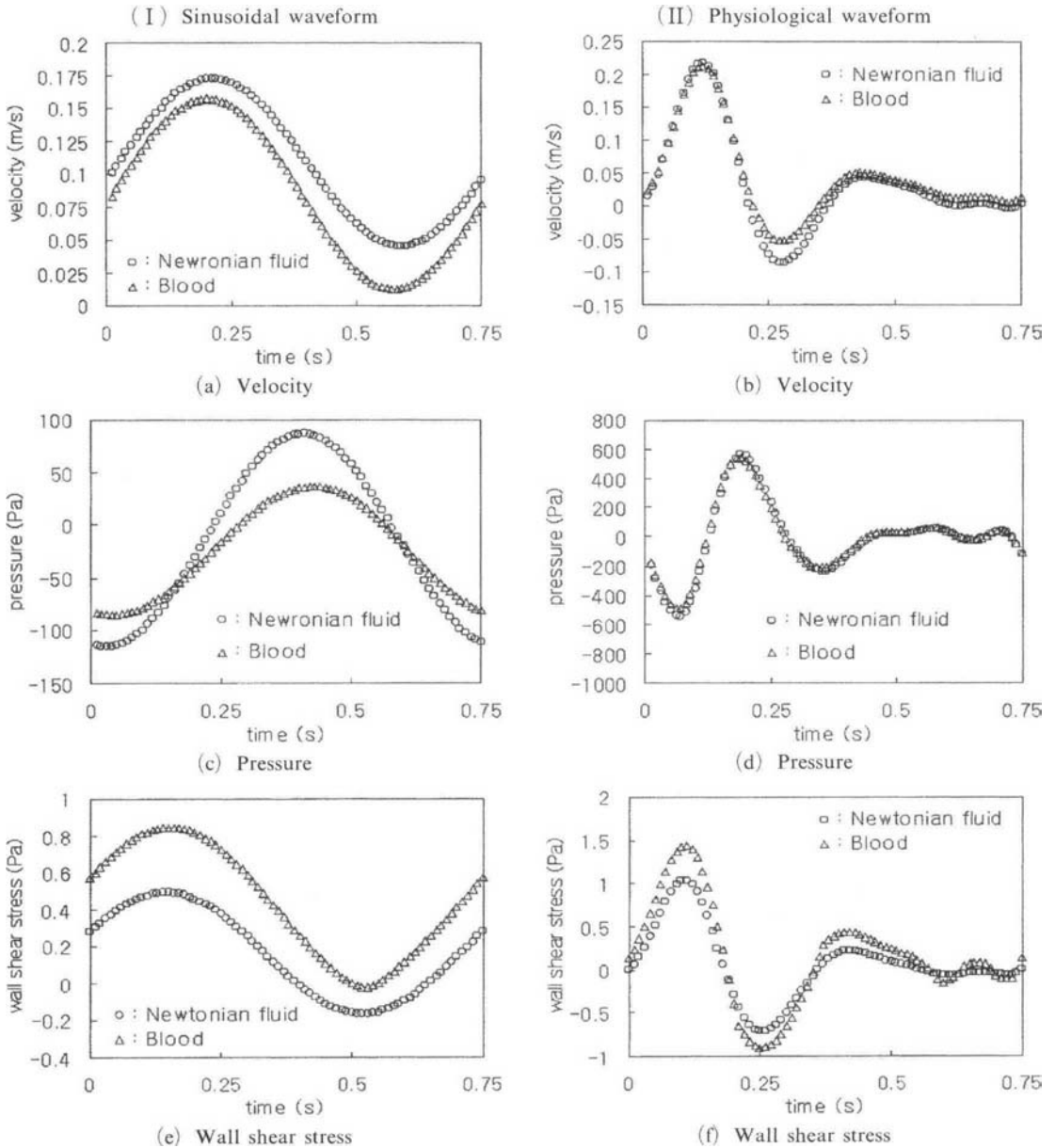


Fig. 15 Comparison of velocity, pressure, and wall shear stresses of two fluids for velocity waveform of $s1$ and $p1$

5. Conclusions

In the present study, effects of the velocity waveform of the physiological flow on the hemodynamics in the bifurcated tube are studied by the using the numerical simulation. The results show as follows ;

For a given sinusoidal velocity waveform at inlet the velocity waveform in a tube approaches the asymptotic waveform after four cycles of the applied velocity waveform in the unsteady flow analysis.

Negative velocity prevails in the developed wall region of the tube during the second deceleration and acceleration phases of the sinusoidal and physiological velocity waveform. Also, the variational tendency of the wall shear stresses along the flow direction is very similar to the applied sinusoidal and physiological velocity waveforms, but the stress values are quite different depending on the local region. In the physiological flow, during deceleration phase waveforms behave differently showing big difference among different waveforms. These phenomena imply that the velocity gradient is dominant factor during acceleration phase and the peak values of the velocity waveform is prevalent factor during deceleration phase. These change of the wall shear stress in a cycle may be an important factor for the mechano-transduction. Endothelial cells on the wall experience the wall shear stresses during a cycle and biochemical reaction between the blood flow and cells is governed by the wall shear stresses. Therefore, rapidly increment of wall shear stresses by changes of waveforms may strongly press the morphology of endothelial cell. And the endothelial cells may be injured or ruptured by the increased wall shear stress. The tendency of velocity, pressure, and wall shear stress between blood and Newtonian fluid for the sinusoidal and physiological velocity waveforms are different quite. Under the sinusoidal velocity waveform the differences in hemodynamics factors of two fluids are quite large, but the differences under the

physiological velocity waveform are negligibly small.

References

- Benerjee, R. K., 1992, A Study of Pulsatile Flows with Non-Newtonian Viscosity of Blood in Large Arteries, Ph. D. Thesis, Drexel University.
- Biro, G. P. 1982, Compression of Acute Cardiovascular Effects and Oxygen Supply Flowing Haemodilation with Dextran, Stroma-Free Haemoglobin Solution and Fluorocarbon Suspension ; Cardiovascular Res., 16, pp. 194~204.
- CFX 4. 1, User Manual, 1996, AEA Industrial Technology Harwell Lab., United Kingdom.
- Milnor, W. R. 1989, Hemodynamics, 2nd Ed., Williams & Wilkins, Baltimore.
- Nichols, W. W. and O'Rourke, M. F., 1990, McDonald's Blood Flow in Arteries, 3rd Ed., Lea & Febiger, Philadelphia.
- Patankar, S. V., 1980, Numerical Heat Transfer and Fluid Flow, McGraw-Hill, N. Y.
- Rhie, C. M. and Chow, W. L., 1983, "Numerical Study of Turbulent Flow Past an Airfoil with Trailing Edge Separation," AIAA J. Vol. 21, pp. 1527~1532.
- Skalak, R., Keller, S. R. and Secomb, T. W., 1981, "Mechanics of Blood Flow," J. of Biomech. Eng., Vol. 103, pp. 102~115.
- Stone, H. L., 1968, "Iterative Solution of Implicit Approximation of Multidimensional Partial Differential Equations," SIAM J. Numer. Anal. Vol. 5, No. 3, pp. 530~558.
- Yoo, S. S., Suh, S. H., Roh, H. W., Kwon, H. M. and Kim, D. S., 1998, Effects of the Anastomosis Angle and the Bypass Diameter on the Aorto-Coronary Bypass Grafting, Proc. 4th KSME-JSME Fluids Eng. Conf., Pusan, Korea, pp. 277~280
- Yoo, S. S., Suh, S. H. and Roh, H. W., 1996, "Numerical Simulation of Flows of Non-Newtonian Fluids in the Stenotic and Bifurcation Tubes," KSME Journal, Vol. 10, No. 2, pp. 223~224. (in Korea)